ZnO Nano-powders as Chemical Sensor to Malathion Vapor

A. Al-Mohammad[a,*], R. Darwich[a], M. Rukiah[b], S. Abo Shaker[a] and M. Kakhia[a]

[a]Nano-materials Labs, Department of Physics, Atomic Energy Commission of Syria, 17th Nissan Street B.O. Box 6091, Damascus, Syrian Arab Republic

[b]Department of Chemistry, Atomic Energy Commission of Syria, 17th Nissan Street B.O. Box 6091, Damascus, Syrian Arab Republic

(Received November 27, 2012; in final form October 31, 2013)

Thick films of zinc oxide (ZnO) nanopowders have been prepared by high energy ball-milling for various spans of mill time (3–18 h). The morphology and crystal structure of the prepared ZnO powder were characterized by scanning electron microscope and X-ray diffraction. The ZnO thick films were then used to construct a gas sensor for O,O-dimethyl dithiophosphate of diethyl mercaptosuccinate (malathion) at different operating temperatures. The sensor response at 100 ppm of malathion was found to reach a maximum as large as 80 at 6 h of high energy ball-milling, four times larger than that found for ethanol. Scanning electron microscope observation of the granular state and pore size distribution analyses indicated that increasing high energy ball-milling time gave rise especially to an increase in the volume of pores in the pore size range of 6–35 nm. It is suggested that such a change in nanostructure is responsible for the marked promotion of the response to malathion.

DOI: 10.12693/APhysPolA.125.131

PACS 81.16.Be, 84.37.+q, 81.20.Ev, 81.20.Wk, 07.07.Df

1. Introduction

Zinc oxide-based gas sensors are efficient for detecting reducing gases such as hydrogen, ethanol, methane, carbon monoxide, ethylene, etc. These devices are also capable to detecting many other compounds present in vapor states within the atmosphere [1–5]. Thus, in order to be able to use these devices for characterizing various pollutants in the atmosphere, it is necessary to understand their behavior when placed in contact with zinc oxide-based gas sensors [4–9]. The ability to detect organophosphorous compounds is very important since these compounds are widely used as insecticides and sometimes as chemical warfare gases.

Malathion (O,O-dimethyl dithiophosphate of diethyl mercaptosuccinate) is a pesticide that is widely used in agriculture, residential landscaping, public recreation areas, and in public health pest control programs such as mosquito eradication. The detection of organophosphorous compounds such as dimethyl methyl phosphonate (DMMP), using a semiconductor has been studied previously [9–12]. Studies on the interaction of various organophosphorous compounds (DMMP, DMHP, TMP, ...) with TiO_2 and WO_3 have also been published recently [12–17]. It appears, however, that the reaction mechanism of the detection of malathion with zinc oxide-based gas sensors has not yet been explored. The origin of this study is that zinc oxide-based gas sensors make it possible to detect malathion vapors in air.

In this article, ZnO nanopowder was prepared by high energy ball milling (HEBM) method. The high resolution X-ray diffraction (XRD) and scanning electron microscope (SEM) techniques were used to characterize nanostructure and morphology of films. We study the response obtained for malathion vapor detection using zinc oxide-based gas sensors and compare it with ethanol. The response of malathion as a function of grain size of the ZnO nanopowders (NPs) was determined. The interaction between the malathion and the zinc oxide samples within a temperature range of 350–700 K has been suggested.

2. Experimental

Commercial ZnO powder (ZnO, $\approx$ 99% purity) was used as a raw material for synthesis of the ZnO nanopowder. ZnO powder was milled by HEBM (Activator 2S, Russia) system with tungsten carbide jars and balls during time from 3 to 18 h with step of 3 h. The milling conditions and the material compositions are summarized in Table.

TABLE

Milling conditions in the high energy ball mill.

Raw materials	Materials of jars & balls	Powder to ball weight ratio	Volumes of jars [ml]	Ball diameters [mm]	Disc speed [rpm]	Jar speed [rpm]
ZnO	WC	1:20	80	10	500	900

The ZnO nanopowder was mixed with water to make paste, which were printed on the (111) silicon substrate 20 mm $\times$ 20 mm $\times$ 0.5 mm patterned by Au electrodes. The thick films were then dried at 550 K for 1 h in air atmosphere.

Malathion was obtained as commercial form with 95% purity. Its characteristics are:

- CAS number: 121-75-5;

*corresponding author; e-mail: pscientific@aec.org.sy

- density: 1.23 g/cm^3;
- molecular mass: 330.358021 g mol^{-1}.
- empirical formula: $C_{10}H_{19}O_6PS_2$;
- boiling point: 156 to 157 K (760 mm Hg).

The powder X-ray diffraction patterns of ZnO nanopowder were carried out using a STOE transmission Stadi-P diffractometer with monochromatic Cu $K_{\alpha 1}$ radiation ($\lambda = 1.5406$ Å). The wavelength was selected using an incident-beam curved-crystal germanium Ge(111) monochromator with a linear position-sensitive detector (PSD). The patterns were scanned over the angular range 20–90° (2θ) with a step length of the PSD of 0.5° (2θ) and a counting time of 30 s per step. The powder samples were loaded between two mylar foils and fixed in the sample holder with a mask of 8.0 mm internal diameter. Scanning electron microscope SEM (TESCAN VIGA II XMU) was used for morphological, crystallite size and nanostructural studies.

Conventionally, the electrical resistivity measurements and the gas-sensing experiments were carried out in a gas flow apparatus equipped with an external controlled heating facility. The resistances of the thick films were measured by the two probes method and using interdigitated gold electrodes deposited on the films by thermal deposition method (Elltrorava, Italy). The nature of the contact was verified to be ohmic by I–V measurements. A thermocouple was attached to the thick films holder for monitoring and controlling the operation temperature during resistance measurements. For each gas measurement experiment a measured quantity of gas at 100 ppm concentration was introduced in the housing and the electrical resistance of each thick film device was measured continuously on an electrometer. Sensor response was defined as the resistance ratio, R_a/R_g, where R_a and R_g stand for the electrical resistances in dry air and the sample gas, respectively.

3. Results and discussion

The X-ray powder diffraction patterns for ZnO raw material and milled powder are shown in Fig. 1. The X-ray patterns indicate that ZnO crystalize in hexagonal (wurtzite) crystal structure with space group ($P63mc$) and cell parameters ($a = 3.249$ Å and $c = 5.205$ Å) [4, 5]. Figure 1 does not show any change in the crystal structure during the milling of the powder. During milling the grain size of ZnO powder change considerably. X-ray patterns show a gradual broadening and simultaneous decrease in intensity of the lines; characteristic of the rapid decrease of grain size of ZnO to nanosized powders (from about 200 nm in raw material to about 30 nm after 3 h milling). The size of ZnO nanocrystallites was evaluated based on diffraction peaks of (100), (002) and (101) by using Scherrer's equation, and their mean values were adopted as an average crystallite size (diameter D).

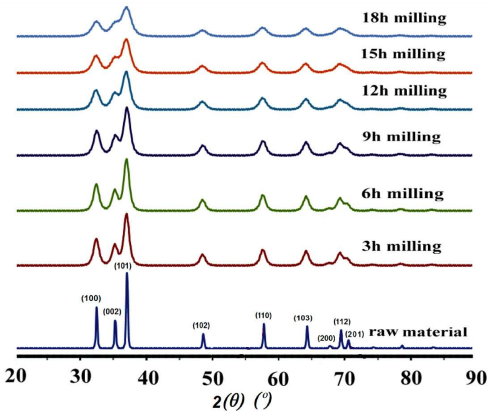

Fig. 1. X-ray diffraction patterns at selected milling times for the ZnO sample milled at 500/900 rpm in comparison with raw material of ZnO.

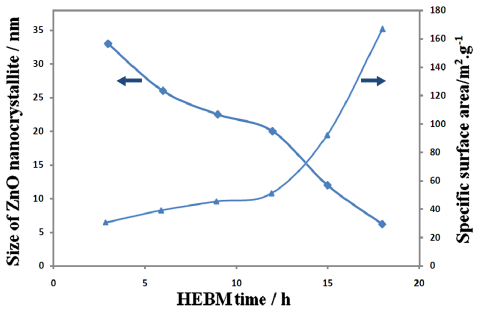

Fig. 2. Size of ZnO nanocrystallite (♦) specific surface area (▲) of ball-milled composites as correlated with HEBM time.

Figure 2 shows the obtained values of D together with the specific surface area (S) data as a function of HEBM time.

The diameter D decreases only slightly with increasing HEBM time, varying from about 33 nm to 6 nm. In contrast, S increases gradually from 32 to 171 m^2/g. These results indicate that the HEBM-induced promotion of sensor response is not only related with the change of D. The change of nanostructure of the grain size of films then draws attention.

Figure 3 shows the SEM images of the thick films of ZnO milled at different times.

The films consist of ZnO grains of various sizes ranging from about 33 nm to 15 nm tended to increase (about 50 nm) with increasing HEBM time. Considering the crystallite sizes shown in Fig. 3 and that calculated from XRD patterns (Fig. 2), most of the grains are agglomerates consisting of two or more crystallites. Changes in morphology with HEBM time (Fig. 3), however, were not always obvious so that pore size (PS) distributions were changed for each period times of milling [17–22].

The sensor response values (R_a/R_g) to 100 ppm of malathion in the temperature range from 350 to 700 K at different HEBM times are shown in Fig. 4.

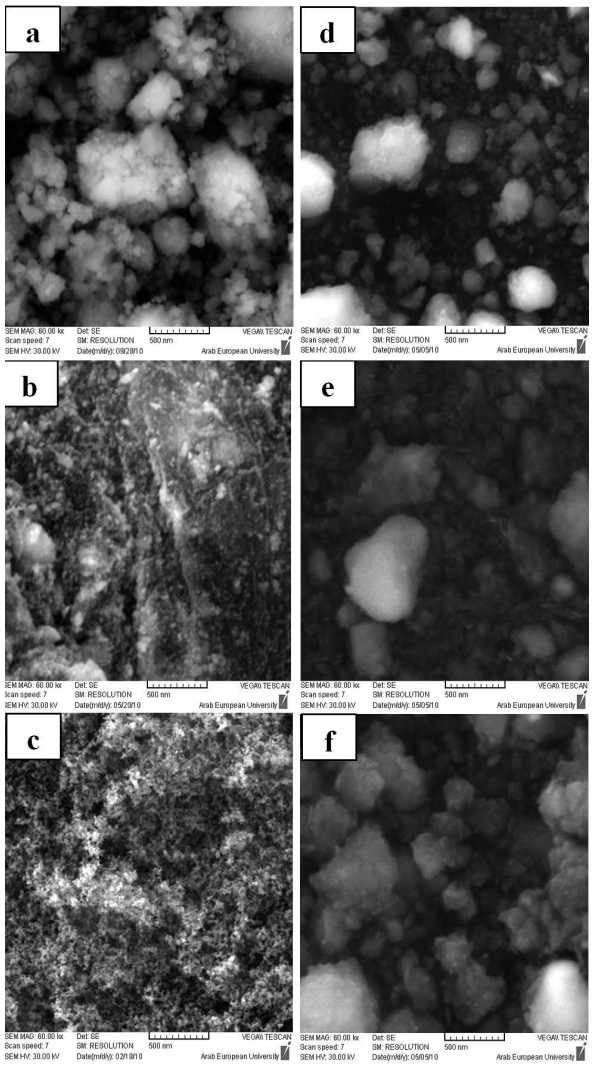

Fig. 3. SEM images of ZnO thick films using ball--milled nanocrystallites. Ball milling time: (a) 3 h, (b) 6 h, (c) 9 h, (d) 12 h, (e) 15 h, (f) 18 h.

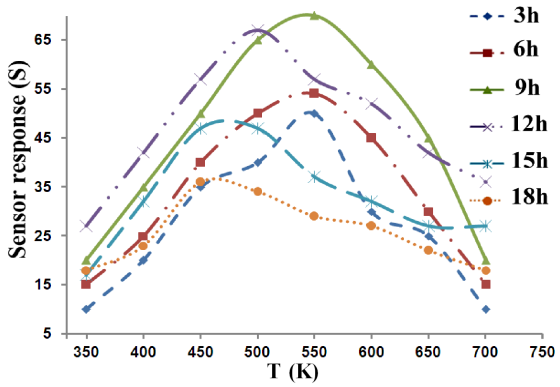

Fig. 4. Sensor response $S = (R_a/R_g)$ to 100 ppm of malathion with operating temperature for different HEBM times.

With HEBM for 3 h, the sensor response versus temperature correlation lays at the lowest position with a rather modest maximum at 550 K among those measures. With increase of the HEBM the correlation shifted upward especially in the higher temperature region, resulting in a monotonously decreasing function of temperature. This tendency continued up to a HEBM time of 9 h, beyond which the correlations began to shift down. The responses at 500 and 550 K are seen to increase sharply especially between 9 and 12 h of HEBM time and then to tend to decrease.

In this way, HEBM for an adequate time (between 9 and 12 h) was very effective in promoting the sensor response especially at the temperature between 500 and 550 K. In order to confirm the performance of our films as sensing element for different gases we compare in Fig. 5 the sensitivity of our films to malathion with that to ethanol. Figure 5 shows that the sensitivity to malathion is three to four times larger than that for ethanol for film obtained at 18 h of milling time. In comparison of earlier results [23–25] on ethanol, our films show also a good performance on ethanol sensing.

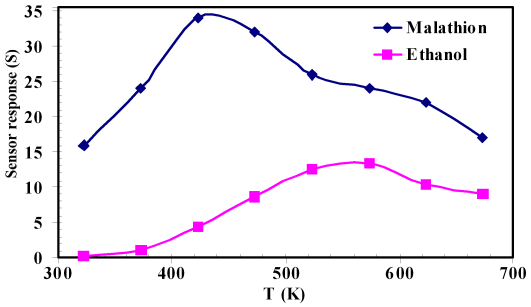

Fig. 5. Comparison between malathion and ethanol gas response for film obtained at 18 h of milling time.

Most semiconducting oxide gas sensors operate on the basis of the modification of the electrical properties of an active element brought about the absorption of an analyte on the surface sensor. When ZnO films sensor is exposed to air, an oxygen molecule absorbs on the surface and forms $O^{\delta-}$ (O_2^-, O^-, O^{2-}) ion [23] by capturing an electron from the conduction band. So ZnO films show a high resistance in air ambient. When ZnO sensor is exposed to reductive gas at moderate temperature, the gas reacts with the surface oxygen species, which decreases the surface concentration of O_2^- ion and increases the electron concentration. Malathion will decompose rapidly when heated to temperature above 375 K. The decomposition is dependent on time as well as temperature due to the exothermic and autocatalytic reactions. The reactions involve rearrangements and polymerization resulting volatile malodorous and inflammable compounds such as ethanol, methanol, and dimethyl sulfide. When these inflammable compounds react with oxygen, a complex series of reactions take place, ultimately converting to carbon dioxide, hydrogen sulfide as

$$\mathrm{CH_3{-}CH_2{-}OH(gas)} + 6\mathrm{O^{2-}} \rightarrow 2\mathrm{CO_2(gas)} + 3\mathrm{H_2O(gas)} + 12\mathrm{e^-},$$

$$\mathrm{CH_3{-}OH(gas)} + 3\mathrm{O^{2-}} \rightarrow \mathrm{CO_2(gas)} + 2\mathrm{H_2O(gas)} + 6\mathrm{e^-},$$

$$\mathrm{CH_3{-}S{-}CH_3(gas)} + 6\mathrm{O^{2-}} \rightarrow 2\mathrm{CO_2(gas)} + 2\mathrm{H_2O(gas)} + \mathrm{H_2S} + 12\mathrm{e^-}.$$

This shows an n-type conduction mechanism in ZnO surface films. Thus on oxidation, single molecule of malathion liberates at least 30 e^- in conduction band and results in increase in conductivity of the sensor. This increase of conductivity of the sensor is more than 2.5 times that for single ethanol molecule. Then if the interaction is due only to the ethanol radical the 100 ppm of malathion must be equivalent to 200 ppm of ethanol. The value of malathion sensor response observed in our work is very high compared to ethanol value at 200 ppm obtained by Wang et al. [23]. This indicates that another radical of phosphor or sulfur in malathion can participate to the interaction with oxygen. Finally, the increase of malathion gas response with milling time can be explained by the increase of the specific surface area in the sense of that the increase of the surface area increases the number of oxygen molecules absorbed on the surface.

4. Conclusions

The thick-film devices using ZnO nanopowder prepared from the ZnO oxide as micropowder by HEBM were promoted markedly for the sensor response to malathion when HEBM time was set adequately (between 9 and 12 h). The promotion of the response to malathion resulted from the change from micro- to nanostructure. This change increased the porosity of ZnO powder by HEBM which increased the global nanopowder surfaces. After 12 h of HEBM the nanopowder became consisting of two or more nanograins and the nanopowder size increased which produced decrease in the malathion response. A mechanism of the interaction explaining the sensor response has been proposed.

References

[1] G.-S. Kim, Y.J. Lee, D.-G. Kim, Y.D. Kim, *J. Alloys Comp.* **454**, 327 (2008).

[2] D.-G. Kim, K.H. Min, S.-Y. Chang, S.-T. Oh, C.-H. Lee, Y. D. Kim, *Mater. Sci. Eng. A* **399**, 326 (2005).

[3] A. Al Mohammad, *Phys. Status Solidi A* **205**, 2880 (2008).

[4] C.V. Ramana, S. Utsunomiya, R.C. Ewing, C.M. Julien, U. Becker, *J. Phys. Chem. B* **110**, 10430 (2006).

[5] H. Meixner, J. Gerblinger, U. Lampe, M. Fleischer, *Sensors Actuat. B* **23**, 119 (1995).

[6] Z.G. Huang, Z.P. Guo, A. Calk, D. Wexler, C. Lukey, H.K. Liu, *J. Alloys Comp.* **422**, 299 (2006).

[7] G.-H. Lee, S.H. Kang, *J. Alloys Comp.* **419**, 281 (2006).

[8] M.C. Yang, J. Xu, Z.Q. Hu, *Int. J. Refractory Metals Hard Mater.* **22**, 1 (2004).

[9] Z. Xiong, G. Shao, X. Shi, X. Duan, Li Yan, *Int. J. Refractory Metals Hard Mater.* **26**, 242 (2008).

[10] A. Al Mohammad, *Vacuum* **83**, 1326 (2009).

[11] A. Galembeck, O.L. Alves, *Thin Solid Films* **365**, 90 (2000).

[12] S. Sathyamurthy, K. Salama, *Physica C* **34**, 2479 (2000).

[13] A. Al Mohammad, F. Maksoud, *Adv. Mat. Res.* **342**, 141 (2012).

[14] O.K. Tan, W. Zhu, Q. Yan, L.B. Kong, *Sens. Actuat. B* **65**, 361 (2000).

[15] O.K. Tan, W. Cao, W. Zhu, *Sens. Actuat. B* **63**, 129 (2000).

[16] Z. Ling, C. Leach, *Sens. Actuat. B* **102**, 102 (2004).

[17] S. Abe, U.-S. Choi, K. Shimanoe, N. Yamazoe, *Sens. Actuat. B* **107**, 516 (2005).

[18] V. Guidi, M. Blo, M.A. Butturi, M.C. Carotta, S. Galliera, A. Giberti, C. Malagù, G. Martinelli, M. Piga, M. Sacerdoti, B. Vendemiati, *Sens. Actuat. B* **100**, 277 (2004).

[19] M. Gillet, K. Aguir, C. Lemire, E. Gillet, K. Schierbaum, *Thin Solid Films* **467**, 239 (2004).

[20] C. Cantalini, W. Wlodarski, Y. Li, *Sens. Actuat. B, Chem.* **64**, 182 (2000).

[21] D.W. Bullett, *J. Phys. C, Solid State Phys.* **16**, 2197 (1983).

[22] C. Scott, S. Ding, R.J. Lad, *Sens. Actuat. B* **77**, 375 (2001).

[23] L. Wang, Y.I. Kang, X. Liu, S. Zhang, W. Huang, S. Wang, *Sens. Actuat. B* **162**, 237 (2012).

[24] Q. Wan, Q.H. Li, Y.J. Chen, T.H. Wang, X. Li, J.P. Li, C.L. Lin, *Appl. Phys. Lett.* **84**, 3654 (2004).

[25] M.Z. Ahmad, A.Z. Sadek, K. Latham, J. Kita, R. Moos, W. Wlodarski, in: *Sens. Actuators B* **187**, 295 (2013).